The effect of alkalinity and temperature on the performance of lithium-air fuel cell with hybrid electrolytes

Ping He, Yonggang Wang, Haoshen Zhou *

Energy Technology Research Institute, National Institute of Advanced Industrial Science and Technology (AIST), Umezono 1-1-1, Tsukuba, 305-8568, Japan

ABSTRACT

A lithium-air fuel cell combined an air cathode in aqueous electrolyte with a metallic lithium anode in organic electrolyte can continuously reduce O_2 to provide capacity. Herein, the performance of this hybrid electrolyte based lithium-air fuel cell under the mixed control of alkalinity and temperature have been investigated by means of galvanistatic measurement and the analysis of electrochemical impedance spectra. Electromotive force and inner resistance of the cell decrease with the increase of LiOH concentration in aqueous electrolyte. The values ranged from 0.5 to 1.0 M could be the suitable parameters for the LiOH concentration of aqueous electrolyte. Environment temperature exhibited a significant influence on the performance of lithium-air fuel cell. The lithium-air fuel cell can provide a larger power at elevated temperature due to the decrease of all resistance of elements.
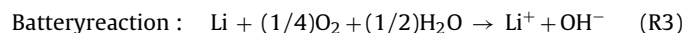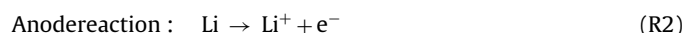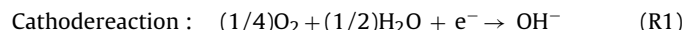
© 2011 Elsevier B.V. All rights reserved.

1. Introduction

Metal-air batteries, such as zinc-air batteries, Mg-air batteries and Al-air batteries, have been extensively studied for a long period [1–4]. The essential advantage of this system is to use inexhaustible oxygen in air as reagent, rather than carry the necessary chemicals around inside the battery, which results in a high energy density. Metallic lithium is the most negative metal while at the same time possessing an ultrahigh capacity of 3860 mAh g^{-1}, thus facilitating the design for higher energy density. The first lithium-air battery with organic electrolyte was introduced in 1996, it had attracted extensive interests due to its superior energy density, which is originated from large free energy for the reaction of metallic lithium with oxygen [5]. At a nominal potential of about 3 V, the theoretical specific energy of the Li-air battery is around 3500 Wh kg^{-1} for the reaction forming Li_2O_2 ($2Li + O_2 \leftrightarrow Li_2O_2$). However, this kind of lithium-air battery is suffered from the diffusion of oxygen, carbon dioxide and water through the electrolyte and their subsequent reaction with metallic lithium. Furthermore, the discharge product Li_2O_2 is not soluble in organic electrolyte, and clogs porous air electrode gradually, which deteriorates the battery performance [5–10].

Recently, a hybrid electrolyte, by uniting air cathode in aqueous electrolyte and a metallic lithium anode in organic electrolyte with a water-stable lithium super ionic conductor glass (LISICON)

plate, was proposed to circumvent the problems of the Li-air battery only using organic electrolyte [10,11]. According to our previous study, the preferred direction of the lithium-air system should be regarded as a fuel cell rather than a rechargeable battery [10,12]. Subsequently, to protect the LISICON plate from being destroyed in strong alkaline electrolyte, a recycle aqueous electrolyte system had also been developed [12]. The O_2 reduction in aqueous solution differs from that in organic solution. OH^-, the O_2 reduction product, can be soluble in aqueous solution instead of being obstacle in porous air electrode in organic electrolyte. This lithium-air fuel cell can provide a high theoretical energy density of 5698 W kg^{-1}, which is higher than that of the rechargeable Li-air battery with organic electrolyte (3500 Wh kg^{-1}) [10]. The electrodes reactions within this lithium-air fuel cell can be described as followed similar to our previous work:

Cathode reaction : $\quad (1/4)O_2 + (1/2)H_2O + e^- \rightarrow OH^-$ (R1)

Anode reaction : $\quad Li \rightarrow Li^+ + e^-$ (R2)

Battery reaction : $\quad Li + (1/4)O_2 + (1/2)H_2O \rightarrow Li^+ + OH^-$ (R3)

During the discharge process, O_2 from air continuously diffuses into the porous air catalytic electrode where electrocatalytic reduction reaction takes place. Simultaneously, Li^+, the oxidation product of lithium metal in organic electrolyte, diffuses across the LISICON plate to form the product LiOH. Considering the reaction (R3), the OH^- concentration can affect the energy and power of lithium-air fuel cell directly through following three aspects: (i) the thermodynamic potential of oxygen reduction; (ii) the catalytic activity of air catalytic electrode; (iii) solution conductivity. On the other
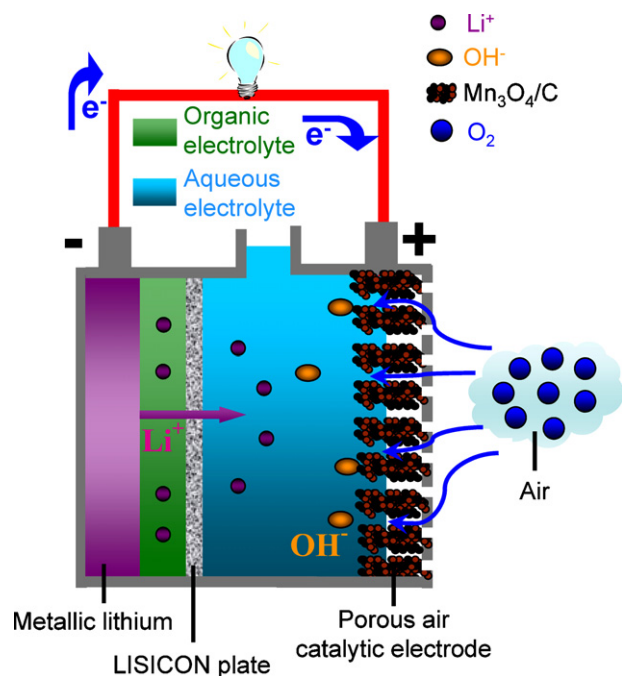
Fig. 1. A schematic representation of the lithium-air fuel cell with hybrid electrolyte.

hand, environment temperature also has a significant impact on the cell system. However, there have been few systematic studies and a lack of understanding on the performance of this lithium-air fuel cell influenced by the alkalinity and temperature. Herein, we systematically studied for the first time the effects of alkalinity and temperature on the performance of lithium-air fuel cell with a structure of Li|organic electrolyte|LISICON plate|LiOH aqueous electrolyte|Mn_3O_4/C catalytic electrode by means of electrochemistry.

2. Experimental

The preparation of Mn_3O_4/activated carbon composite used as catalytic electrode is given in previous report [13]. The catalyst material contains Mn_3O_4 (25 wt.%) and active carbon (75 wt.%). The air catalytic electrode includes a catalyst layer and a gas diffusion layer. The prepared Mn_3O_4/carbon composite (85 wt.%) and polytetrafluoroethylene (PTFE) (15 wt.%) were well mixed, and then was roller-pressed into a sheet to form catalytic layer. The gas diffusion layer was prepared by mixing acetylene black (60 wt.%) and PTFE emulsion (40 wt.%) with isopropanol into paste and then rolling the paste into a film. The air catalytic electrode was finished by pressing the catalyst layer and gas diffusion layer onto a nickel mesh. The area of the air electrode was $1 cm^2$, and the mass load of catalyst layer was $4.5 mg cm^{-2}$.

The structure of developed lithium-air fuel cell was shown in Fig. 1 and can be described as: (1) the organic electrolyte (1 M $LiClO_4$ in ethylene carbonate/dimethyl carbonate) and LiOH aqueous electrolyte are separated by a LISICON plate. (2) The organic electrolyte is just a thin liquid layer (or electrolyte adsorbed by porous membrane) that is used to separate wet metallic Li-anode and LISICON plate. (3) The air catalytic electrode combining catalyst layer with the gas diffusion layer is located between aqueous electrolyte solution and air atmosphere. The area of Li anode is about $2 cm^2$. The distance between Li anode and air electrode is about 4 cm and the cell contains 5 ml aqueous electrolytes. The catalyst layer contacts the aqueous electrolyte while the gas diffusion layer faces the air atmosphere. The used LISICON plate is provided by Ohara Inc., Japan. The thickness of LISICON plate is 150 μm. The

electrical conductivity of the LISICON plate is about $4 \times 10^{-4} S cm^{-1}$ at room temperature.

Electrochemical tests were performed using a Solartron 1287 Electrochemical Interface and a Solartron 1255B Frequency Response Analyzer, and controlled by Corrware and Z-plot from a PC. For the electrochemical impedance spectra (EIS) test metallic lithium was used as the counter and reference electrode. The frequency limits were typically set between 10 kHz and 0.01 Hz. The AC oscillation was 10 mV. The obtained data of EIS were fitted from equivalent circuit using Zview 2.70 software.

3. Results and discussion

3.1. The performance of Li-air fuel cell in various alkalinity aqueous electrolytes

The Li-air fuel cell with acidic aqueous solution has a higher operating voltage comparing with that in neutral and basic electrolyte, which results in a larger energy density. However, only expensive noble metal such as Pt and Pd can be used as catalytic electrode in this acidic environment. So, the acidic electrolyte based Li-air fuel cell is hardly practical for industrial generalization until the substitution of noble metal has been developed. In our experiment, a Mn_3O_4/activated carbon composite material was selected as catalyst in LiOH alkaline electrolyte based Li-air fuel cell due to its low cost and high activity.

The concentration of LiOH solution ranged from 0.01 to $2.0 mol L^{-1}$. Fig. 2 gives a series of relations between operating voltage (power density) and applied current density in various concentration of LiOH aqueous electrolyte. As seen in Fig. 2, with the growth of applied current densities, linear decrease of operating voltage is clearly observed. For a battery system, the decrease in operating voltage with increasing current density is considered to be caused by a combination of kinetic, transport, and ohmic limitations in system. The drop from the kinetic limitation is relatively small compared to the other drops in the system and hence any error in this would be negligible [14]. In our case, the electrochemical reactions ((R1) and (R2)) take place at the interface between solid electrode and liquid electrolyte instead of a intercalation reaction. Thus it is not necessary to consider the transport limitation in the solid phase. We are still left with analyzing the ohmic limitation for the decrease in the operating voltage. The ohmic limitation is mainly consisting of solution resistance (the resistance of liquid solution and LISICON plate), contact resistance (resistance between the current collector and the porous electrode) and matrix resistance (resistance between the current collector end of the porous electrode and electrode/electrolyte interface through the matrix phase) [14]. As we know, the operating voltage (U) can be expressed as followed formula:

$$U = E - I \times R \tag{1}$$

where E is the electromotive force which is related with the chemical component of active electrodes and electrolyte, I is the applied current, R is the inner resistance of the fuel cell and mainly consisting of the solution resistance, contact resistance and matrix resistance. As seen from this formula, the operating voltage linear decrease with increase of applied current, which is consistent with the experimental phenomenon displayed in Fig. 2. The inner resistance of fuel cell was estimated from the decline rate of linear curves. The electromotive force (E) obtained from the OCV of Li-air batter and inner resistance (R) with various LiOH concentration and environmental temperature were summarized in Table 1. According to the data displayed in Table 1, E decreases with increase of concentration of LiOH in aqueous electrolyte. The OCV potential of this Li-air hybrid cell can be relative to the reversible poten-
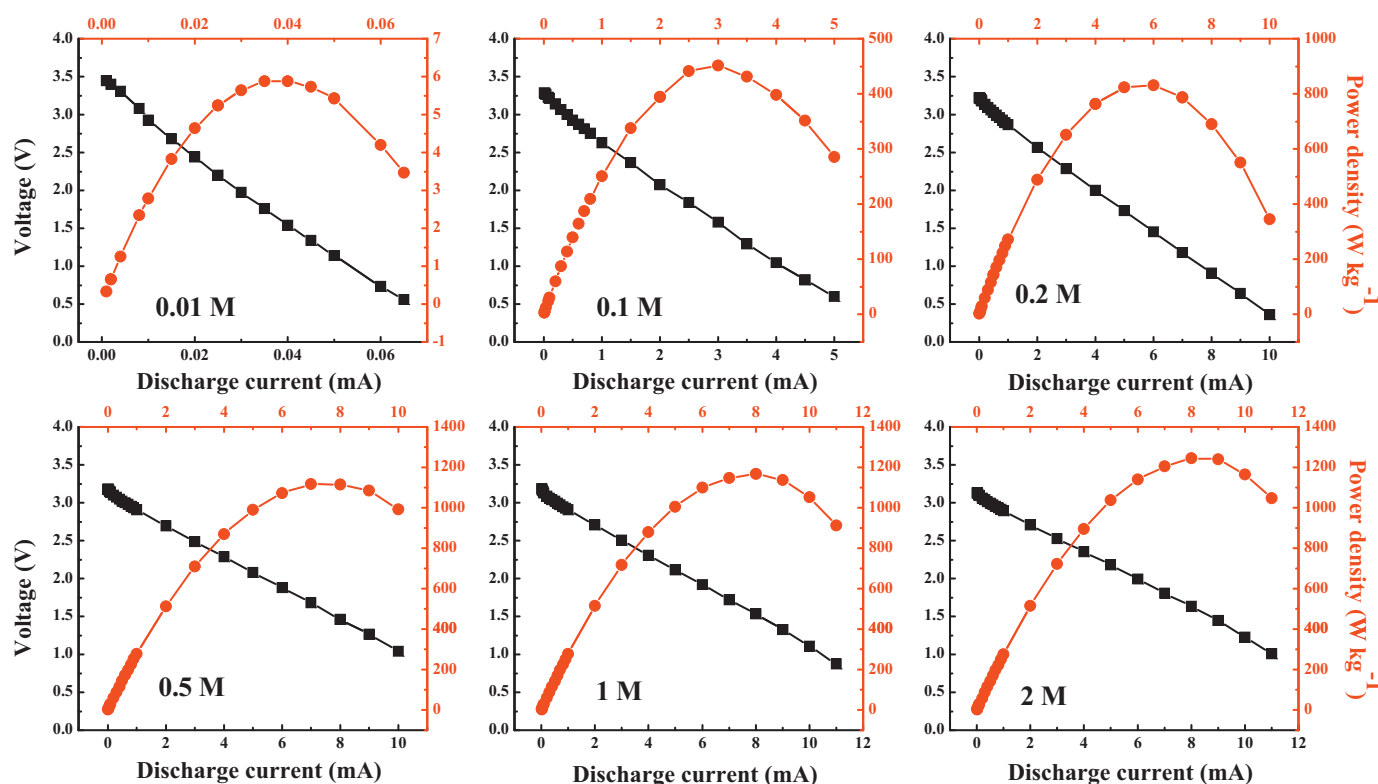
Fig. 2. The relations between operating voltage (power performance) and applied current density in various concentration of LiOH aqueous electrolyte.

Table 1
Electromotive force (E) and inner resistance (R), with various LiOH concentration and environmental temperature.

	Temperature							
	25 °C						40 °C	55 °C
LiOH concentration (M)	0.01	0.1	0.2	0.5	1	2	1	1
E (V)	3.46	3.30	3.25	3.20	3.19	3.16	3.21	3.23
R (Ω)	4390	525	278	204	200	185	165	148

tial of OH^-/O_2, which obeys the Nernst equation. So OCV potential decreases with increase of OH^- concentration in our experimental. The inner resistance (R) also decreases with increase of concentration of LiOH in aqueous electrolyte. The larger inner resistance of cell with the LiOH concentration lower than 0.1 M is mainly due to the low conductance of aqueous electrolyte. It is suggested that the LiOH concentration has the significant impact on both the electromotive force and inner resistance. This phenomenon is reasonable because that the OH^- ion take a role of not only the reaction product (see (R1)) but also the supporting electrolyte.

As we know, the output power (P) of the cell can be expressed as followed:

$$P = I \times U = I \times (E - I \times R) = -I^2R + I \times E \qquad (2)$$

$$P_{max} = \frac{E}{2R} \qquad (3)$$

where definitions of I, r, U and E are same as that of formula (1). Derived from formula (2), the output power (P) should have a maximum value at the applied current of $E/2R$. In other words, with the increase of applied current densities the power can increase and then decrease. Apparently, the maximum power depends on the LiOH concentration in aqueous electrolyte. Fig. 3 gives the measured maximum power density of Li-air fuel cell in various LiOH concentrations. This calculation of power density is based on the total mass of catalytic electrode in order to facilitate comparison,

which was adopted in all previous reports [10,12]. Herein, the calculation method of power density does not affect the results of our discussion. As seen in Fig. 3, the maximum power density increase little with the LiOH concentration larger than 0.5 M. Thus increasing the LiOH concentration above 0.5 M is of little effective for
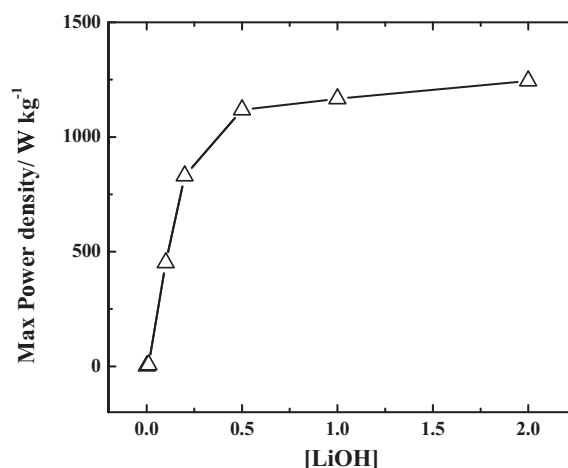

Fig. 3. The variation of maximum power density with different LiOH concentrations.
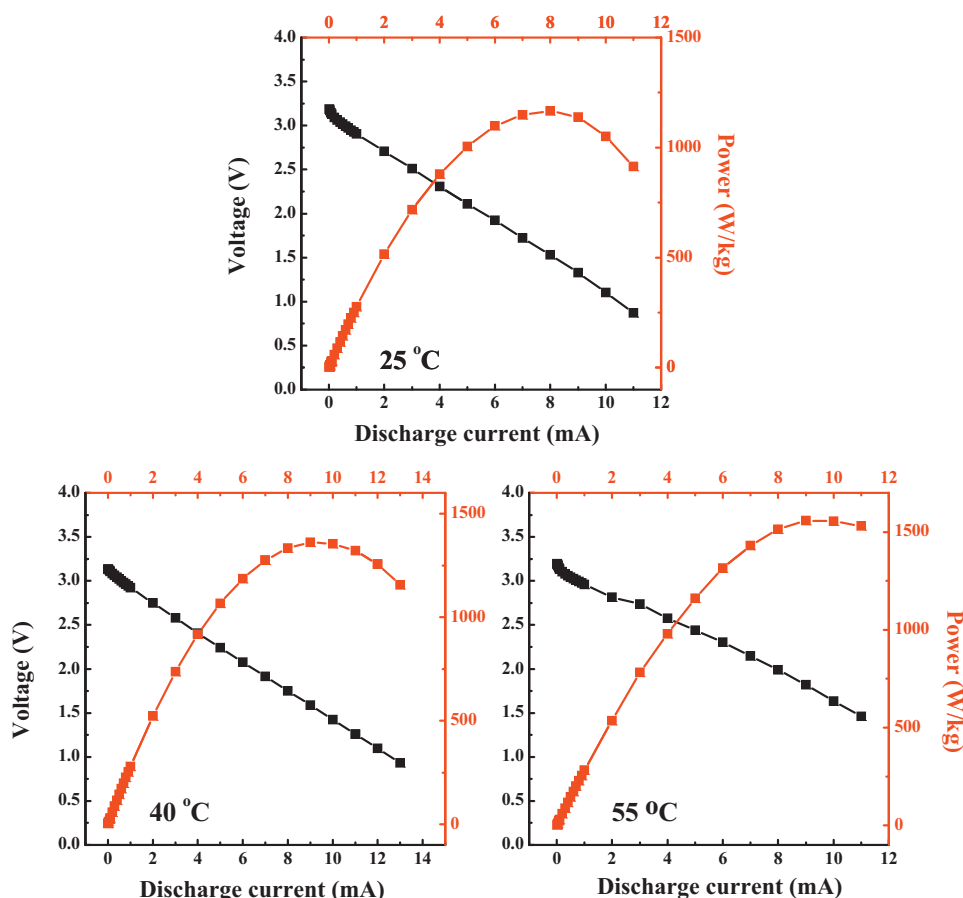
Fig. 4. The variation of voltage and power density with applied current at different temperatures.

enhancing the power. Considering the cost and the weight of cell, the suitable LiOH concentration of aqueous electrolyte ranged from 0.5 to 1.0 M.

3.2. Effect of temperature on the performance of Li-air fuel cell

Now, let us consider the effect of environment temperature on the performance of Li-air fuel cell. Fig. 4 illustrates the variation of voltage and power density with applied current at different temperatures. It was found that the Li-air fuel cell reached a maximum power density of 1166, 1360 and 1556 W kg^{-1} at 25, 40 and 55 °C, respectively. As the temperature elevated the maximum power density increases in value. The maximum power density varies with temperature due to the change of the electromotive force and the inner resistance, which can be derived from the formula (3). The electromotive force (E) of Li-air fuel cell that was measured from OCV shows little changes at various temperatures. Therefore, the increase of the maximum power density with elevating environmental temperature is mainly attributed to the decrease of inner resistance that can be estimated from the slope of linear relation between voltages and applied current. The inner resistances at higher temperatures were also displayed in Table 1. It is suggested that the inner resistance of cell decreases with an increase of temperature. Thus the Li-air fuel cell can provide a larger power at higher temperature, although the operating temperature should not be too high to evaporate the electrolyte.

3.3. Electrochemical impedance spectroscopy of Li-air batteries

As discussed above, it is confirmed that the variation of power performance as the function of alkalinity and environmental tem-

perature was mainly attributed to the inner resistance of the lithium-air fuel cell. Accordingly it seems important to analyze the detailed elements of inner resistance that are influenced by alkalinity and temperature. AC electrochemical impedance spectroscopy (EIS) technique has proven to be reliable and powerful tool for investigation of kinetic processes in cell system. Herein, impedance measurement was carried out with a structure of Li|organic electrolyte|LISICON plate|LiOH aqueous electrolyte|Mn$_3$O$_4$/C catalytic electrode. Nyquist plots of the Li-air fuel cell with air catalytic electrode in various concentrations LiOH are shown in Fig. 5. The impedance spectra were analyzed using equivalent circuits with resistive (R_i)/capacitive (C_i) combination and the respective circuit elements were deduced by fitting the experimental data points with the circuit shown in Fig. 6. R_e represents the resistance attributed to the electrolyte and cell components (including bulk resistance of LISICON plate and porous electrode etc.); the semicircle in high frequency can be ascribed to grain boundary resistance in the LISICON and air porous electrode (denoted as R_{gb}); the depressed semicircle in high-intermediate frequency is attributed to the interfacial resistance between electrode and electrolyte (denoted as R_{int}); the small semicircle in low frequency arises from charge-transfer resistance (denoted as R_{ct}); W_o is the Warburg diffusion contribution. CPE1, CEP2 and CEP3 are their associated capacitances. The non-homogeneity of the composite electrode system reflected as a depressed semicircle in the impedance response was accounted by considering a constant phase element (CPE) in place of a capacitor (C_i) in the equivalent circuit. Thus, from the impedance of the CPE, $Z = 1/B(j\omega)^n$ ($j = (-1)^{1/2}$, ω is the angular frequency, B and n are constants), the degree of distortion of the impedance spectra can be obtained from the value of n, and at $n = 1$, $B = C_i$, the ideal capacitor. In Fig. 5, the continuous lines
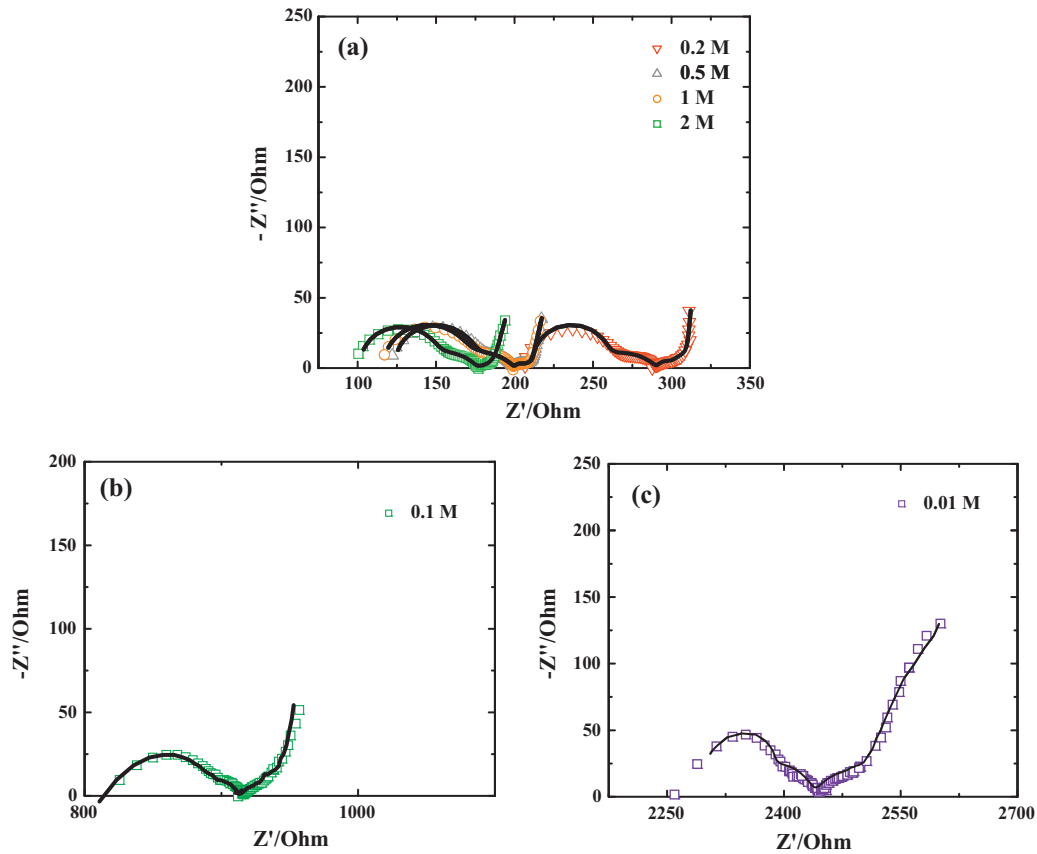
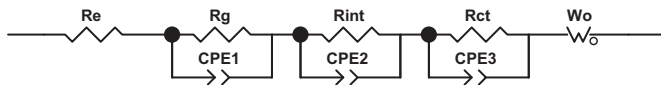**Fig. 5.** Nyquist plots of the Li-air fuel cell with air catalytic electrode in various concentrations LiOH.

Fig. 6. Equivalent circuit used to fit the experimental data. R_e represents the resistance attributed to the electrolyte and cell components; R_{gb} is the grain boundary resistance in the LISICON and air porous electrode; R_{int} is the interfacial resistance between electrode and electrolyte; R_{ct} is the typical charge-transfer resistance (denoted as); W_o is the Warburg diffusion contribution. CPE1, CEP3 and CEP3 are their associated capacitances.

represent the fitting of the equivalent circuit whereas the symbols denote the experimental data points as a function of frequency at OCV. As can be seen the experimental points fitted well with the values calculated from the equivalent circuit. The fitting results of circuit elements in various LiOH concentrations were displayed in Table 2. As seen in Table 2, the resistances of the electrolyte and cell components ranged from 101.2 to 2305.8 Ω with the LiOH concentration decreased from 2.0 to 0.01 M. Simulations also show that no significant changes of the grain boundary resistances in the LISICON and air porous electrode (R_{gb}) were observed in the concentration range, thereby suggesting that alkalinity has little impact on the grain boundary resistance. R_{int} and R_{ct} slightly increase with the

decrease of alkalinity. Lithium ion concentration at solid–liquid interface affect the process of interficial charge transfer. Increasing LiOH concentration facilitate charge transfer at interface. Therefore charge transfer resistance increase when the LiOH concentration decreases. Note that W_o has no obvious changes except for the LiOH concentration lower than 0.1 M. All these results suggest that the LiOH concentration has the greatest impact on the resistance of R_e. We speculate that R_e varying with LiOH concentration arises from the change of conductivity of aqueous electrolyte.

In order to further extract the effect of temperature on the lithium-air fuel cell, the EIS tests were conducted at various temperatures with the LiOH concentration fixed on 1 M. Fig. 7 illustrates the Nyquist plot of the EIS measured experimentally at 25, 40 and 55 °C. The EIS data were also fitted using the equivalent circuit model shown in Fig. 6. Similarly, solid lines represent the fitting data while the symbols denote the experimental data points. Simulated results of EIS data using the equivalent circuit mode at different temperatures were presented in Table 3. It can be seen from the fitting results that all resistance of elements decrease when rising the temperature. It is easy to understand that rising the temperature can enhance the conductivity of liquid and solid electrolyte, which leads to a decrease in R_e. Particularly, LISI-

Table 2
Simulated results for the elements of equivalent circuit in various LiOH concentrations electrolyte.

	R_e/Ω	R_{gb}/Ω	R_{int}/Ω	R_{ct}/Ω	W_o/Ω
2 M	101.2	44.3	36.1	13.6	50.2
1 M	116.7	44.2	37.2	13.9	49.0
0.5 M	124.4	43.9	40.9	14.1	49.3
0.2 M	211.3	43.7	58.5	14.9	51.3
0.1 M	835.7	44.5	81.2	21.8	129.2
0.01 M	2305.8	41.2	123.9	39.7	279.7

Table 3
Simulated results for the elements of equivalent circuit at different temperatures.

	R_e/Ω	R_{gb}/Ω	R_{int}/Ω	R_{ct}/Ω	W_o/Ω
25 °C	116.7	44.2	37.2	13.9	46.0
40 °C	90.3	26.0	19.7	10.2	39.9
55 °C	87.7	9.5	14.7	9.9	0.7
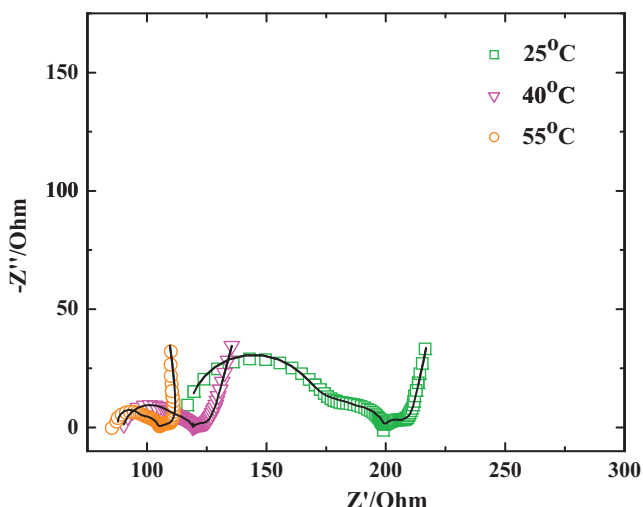
Fig. 7. The Nyquist plot of the EIS measured experimentally at various temperatures.

CON plate, the NASICON-type solid electrolyte, located between organic and aqueous electrolyte plays a role of solid electrolyte. It has been reported that the resistances of grain and grain boundary in NASICON-type solid electrolyte decrease with rise of temperature [15]. The decrease of charge transfer resistance with rise of temperature is attributed to enhanced catalytic activity of catalyst layer at higher temperature. In addition, Warburg diffusion resistance and the interfacial resistance between electrode and electrolyte also have significant decrease with an increase of temperature. Consequently, it is helpful to reduce the inner resistance of cell by elevating temperature, which leads to the enhancement of power performance of Li-air fuel cell. The variation of simulated results using equivalent circuit as a function of LiOH concentration and temperature is consistent with changes of maximum power described above.

4. Conclusion

In this study, we have investigated the performance of hybrid electrolyte based lithium-air fuel cell under the mixed control of alkalinity and temperature by means of galvanistatic measurement and the analysis of AC EIS. The operating voltage of the lithium-air fuel cell has a linear decrease with the growth of applied current densities, which is mainly due to the ohmic limitation. The electromotive force and inner resistance of the cell decrease with the increase of LiOH concentration in aqueous electrolyte. As for the power performance, increase of the LiOH concentration above 0.5 M is of little effective for enhancing the power. Thereby concentration ranged from 0.5 to 1.0 M is considered as the suitable parameters for the LiOH aqueous electrolyte. The environment temperature exhibited a significant impact on the performance of lithium-air fuel cell. The Li-air fuel cell can provide a larger power at elevated temperature due to the decrease of all resistance of elements. This work promotes the practical use of lithium-air fuel cell.

References

[1] J. Chen, F.Y. Cheng, Acc. Chem. Res. 42 (6) (2009) 713.
[2] W.Y. Li, C.S. Li, C.Y. Zhou, H. Ma, J. Chen, Angew. Chem. Int. Ed. 45 (36) (2006) 6009.
[3] S.H. Yang, H. Knickle, J. Power Sources 112 (1) (2002) 162.
[4] G.Q. Zhang, X.G. Zhang, H.L. Li, J. Solid State Electrochem. 10 (12) (2006) 995.
[5] K.M. Abraham, Z. Jiang, J. Electrochem. Soc. 143 (1996) 1.
[6] J. Read, J. Electrochem. Soc. 149 (2002) A1190.
[7] T. Ogasawara, A. Debart, M. Holzapfel, P. Novak, P.G. Bruce, J. Am. Chem. Soc. 128 (2006) 1390.
[8] A. Debart, A.J. Paterson, J. Bao, P.G. Bruce, Angew. Chem. Int. Ed. 47 (2008) 4521.
[9] X.H. Yang, P. He, Y.Y. Xia, Electrochem. Commun. 11 (2009) 1127.
[10] Y.G. Wang, H.S. Zhou, J. Power Sources 195 (2010) 358.
[11] S.J. Visco, E. Nimon, B.D. Katz, 12th International Meeting on Lithium batteries, Nara, Japan, 2004 (Abstracts #397).
[12] P. He, Y.G. Wang, H.S. Zhou, Electrochem. Commun. 12 (2010) 1686.
[13] Y.G. Wang, L. Cheng, F. Li, H.M. Xiong, Y.Y. Xia, Chem. Mater. 19 (2007) 2095.
[14] V. Srinivasan, J. Newman, J. Electrochem. Soc. 151 (10) (2004) A1517.
[15] E. Kazakevičius, A. Určinskas, A. Kežionis, A. Dindune, Z. Kanepe, J. Ronis, Electrochim. Acta 51 (27) (2006) 6199.